

Processing of Poly(lactic-co-glycolic acid) Microfibers via Melt Electrowriting

Christoph Böhm, Biranche Tandon, Andrei Hrynevich, Jörg Teßmar, and Paul D. Dalton*

Polymers sensitive to thermal degradation include poly(lactic-co-glycolic acid) (PLGA), which is not yet processed via melt electrowriting (MEW). After an initial period of instability where mean fiber diameters increase from 20.56 to 27.37 μm in 3.5 h, processing stabilizes through to 24 h. The jet speed, determined using critical translation speed measurements, also reduces slightly in this 3.5 h period from 500 to 433 mm min^{-1} but generally remains constant. Acetyl triethyl citrate (ATEC) as an additive decreases the glass transition temperature of PLGA from 49 to 4 $^{\circ}\text{C}$, and the printed ATEC/PLGA fibers exhibits elastomeric behavior upon handling. Fiber bundles tested in cyclic mechanical testing display increased elasticity with increasing ATEC concentration. The processing temperature of PLGA also reduces from 165 to 143 $^{\circ}\text{C}$ with increase in ATEC concentration. This initial window of unstable direct writing seen with neat PLGA can also be impacted through the addition of 10-wt% ATEC, producing fiber diameters of $14.13 \pm 1.69 \mu\text{m}$ for the first 3.5 h of heating. The investigation shows that the initial changes to the PLGA direct-writing outcomes seen in the first 3.5 h are temporary and that longer times result in a more stable MEW process.

1. Introduction

Melt electrowriting (MEW) is a technique that allows for deposition of fibers in the lower micrometer range in a very precise manner,^[1,2] and poly(ϵ -caprolactone) (PCL) is the current gold standard material.^[3] With its low melting point and slow degradation, PCL can remain being heated for long periods without measurable degradation.^[4] This is essential for a system such as MEW that relies on applying heat to an entire volume of the melt, since an air pressure-type delivery of the molten polymer to the nozzle is important to achieve small diameter fibers.^[5] MEW processing requires a low, stable flow rate to the nozzle while filament-type and screw-driven systems, generally deliver higher flow rates that result in large diameter fiber.^[6] For example, a screw-driven melt electrospinning system reported $360 \mu\text{L h}^{-1}$ as the lowest extrusion flow rate for linear

PCL,^[7] corresponding to 100 μm fiber diameter. This contrasts to a calculated extrusion rate of $1.5\text{--}5 \mu\text{L h}^{-1}$ for 12–25 μm diameter PCL fibers using air pressure.^[4] The smallest diameter MEW fibers produced to date are 0.8 μm and are also made from PCL.^[8]

While polymers have been processed or developed for MEW, thermal degradation or crosslinking limits the library of processable materials.^[3] The viscosity of the melt affects the flow rate to the nozzle and the processing of materials can be challenging as MEW currently requires keeping a material in a sustained molten state, which can change the direct-writing behavior in prolonged processing time frames.


There are several materials that have already been successfully processed with MEW,^[3] many of which are polyesters. These include poly(L-lactide-co- ϵ -caprolactone)^[9] or a 60:40 mixture of PCL and (poly(hydroxymethyl glycolide-co- ϵ -caprolactone) to promote changes in surface wetting or mechanical properties.^[10] Furthermore, 45S5 bioactive glass could be added to a blend of polylactide (PLA) and poly(lactide-*block*-ethylene glycol-*block*-lactide) (PLA-PEG-PLA) and successfully processed via MEW.^[11] Conversely, crosslinking can occur during heating that affects the process stability. Recently, a system of furan and maleimide functionalized poly(2-ethyl-2-oxazine) that crosslink with the help of Diels–Alder reactions was MEW processed which was later peptide-functionalized to enhance the attachment of cells.^[12] There is, however, a limited period of processing due to the crosslinking of the two components in the heated reservoir increasing the viscosity until material flow stops.

C. Böhm, B. Tandon, A. Hrynevich, J. Teßmar, P. D. Dalton
 Department of Functional Materials in Medicine and Dentistry and
 Bavarian Polymer Institute
 University of Würzburg
 Pleicherwall 2, Würzburg 97070, Germany
 E-mail: pdalton@uoregon.edu

B. Tandon, P. D. Dalton
 Knight Campus for Accelerating Scientific Impact
 University of Oregon
 1505 Franklin Blvd, Eugene, OR 97403, USA

A. Hrynevich
 Department of Veterinary Science
 Utrecht University
 Yalelaan 1, CL, Utrecht 3584, Netherlands

A. Hrynevich
 Department of Orthopedics
 UMC Utrecht
 Heidelberglaan 100, CX, Utrecht 3584, Netherlands

 The ORCID identification number(s) for the author(s) of this article can be found under <https://doi.org/10.1002/macp.202100417>

© 2022 The Authors. Macromolecular Chemistry and Physics published by Wiley-VCH GmbH. This is an open access article under the terms of the Creative Commons Attribution License, which permits use, distribution and reproduction in any medium, provided the original work is properly cited.

DOI: 10.1002/macp.202100417

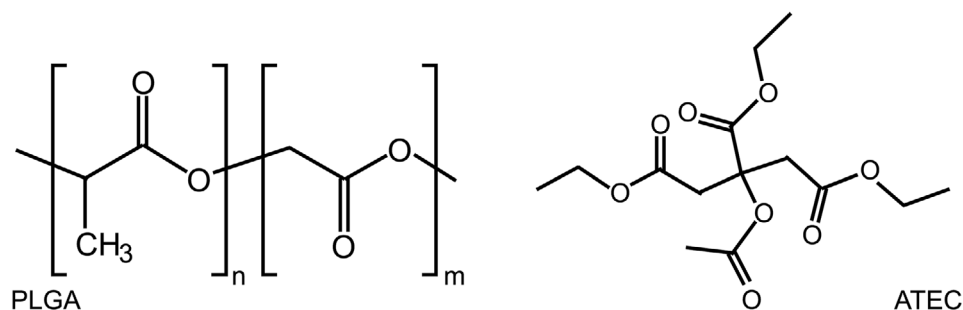


Figure 1. Chemical structure of PLGA and ATEC used in this study.

A potential new polyester to include within the MEW-processable library is poly(lactic-co-glycolic acid) (PLGA). PLGA is a versatile polymer that has a long clinical history and is mostly used as a drug delivery system^[13] or as a scaffold in tissue engineering.^[14,15] The degradation of PLGA is favorable as it undergoes hydrolysis of the ester group in the presence of water to release lactic and glycolic acid over month-long periods. These acids are byproducts of metabolic pathways and can further be metabolized by the Krebs cycle,^[16] which causes minimal toxicity at sufficiently high scaffold porosities.^[15,17] Additionally, it is possible to tune the degradation time frame by changing the initial molecular weight, the ratio of glycolic and lactic acid and the dimensions of the implantable device.^[16]

As beneficial as a controlled degradation rate is for drug release and TE applications, the processability of PLGA with a melt processing technique like MEW can be challenging. In a comparative study of thermal degradation of PCL, polyglycolic acid (PGA) and PLA, Sivalingam et al. showed that PLA and PGA decompose at lower temperatures than PCL.^[18] At a processing temperature of 165 °C for neat PLGA compared to around 85 °C for PCL, PLGA should degrade faster, which will have an influence on the viscosity of the MEW jet material.

Additionally, we investigate the inclusion of acetyl triethyl citrate (ATEC) (**Figure 1**) as a plasticizer for lowering the glass transition (T_g) and direct-writing temperature of PLGA. The increase in flexibility of PLGA fibers due to addition of ATEC is a direct effect often observed in polymers for various plasticizers.^[19,20] Such plasticizers can reduce the tensile strength and Young's modulus of polymers, as well as increase the elastic recovery.^[21] To compare these blends and determine their direct-writing stability, the jet speed was determined, as measured by the critical translation speed (CTS).

2. Experimental Section

2.1. Material

PLGA with a 1:1 lactic to glycolic acid ratio (Evonik Operations GmbH, Darmstadt, Germany, RESOMER RG 505, Lot# D161000569) and an inherent viscosity of 0.73 dl g⁻¹ (25 °C, 0.1%, CHCl₃) was used for all experiments. The material was aliquoted into 50 mL Falcon tubes, purged with argon and stored at -80 °C. The tubes were fully warmed to room temperature prior to opening to prevent condensation of water vapor on the PLGA.

Table 1. Nomenclature used and ratio between PLGA and ATEC for different blends, and the T_{Syringe} and T_{Nozzle} for each formulation.

Blend	PLGA [wt%]	ATEC [wt%]	T_{Syringe} [°C]	T_{Nozzle} [°C]
PLGA	100	0	165	144
PLGA10	90	10	157	136
PLGA20	80	20	155	128
PLGA30	70	30	143	118

ATEC (Sigma Aldrich, St. Louis, USA) was used as plasticizer as received.

2.2. Preparation of the PLGA/ATEC Blends

Different ratios of the PLGA/ATEC blends were prepared according to **Table 1** by using a 25-wt% solution of PLGA in dichloromethane (Thermo Fisher Scientific, Waltham, USA) and adding the respective amount of ATEC. The resulting mixture was vigorously stirred for 3 h before drawing films (COATMASTER 510, ERICHSEN GmbH & Co. KG, Hemer, Germany). The films were air dried overnight, cut into pieces, and further dried under vacuum for 3 h. The blends were stored at -80 °C under argon to prevent degradation.

2.3. MEW Printer

A custom-built MEW printer (**Figure 2**) with SiN ceramic heater (Bach RC, Werneuchen, Germany), a spiral heater (HKE-tec, Pfarrkirchen, Germany), and a brass electrode connected to a high voltage (HV) source (HCP 14-20000, FuG Elektronik GmbH, Schechen, Germany) set to positive polarity was used. Compressed nitrogen was utilized to pressurize the syringe using a valve (Aventics, Laatzten, Germany). The nozzle was positioned above an aluminum collector connected to a second HV source with a negative polarity. The x-y linear axis (Bosch Rexroth AG, Schweinfurt, Germany) of the collector was controlled via G-code run by IndraMotion MTX (Bosch Rexroth AG, Schweinfurt, Germany). To control the ambient conditions of temperature and humidity, the MEW device was enclosed into an airtight casing connected to a climate chamber

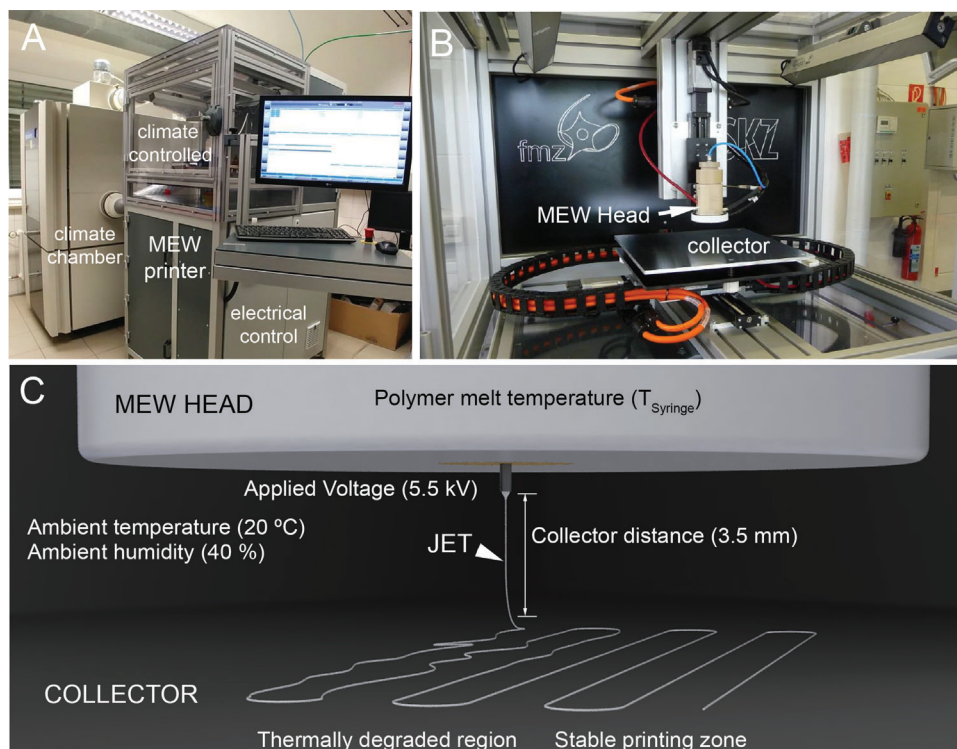


Figure 2. Configuration of the MEW printer and schematic of experiments. Photographs showing A) the configuration of the climate chamber and MEW printer and B) inside the airtight casing of the MEW printer. C) A schematic outlining the important parameters used.

(DM340 C AC, ATT Umweltsimulation GmbH, Ofterdingen, Germany).

2.4. Preparation and Pre-Treatment

The 0 h timepoint was neat, untreated PLGA. MEW was performed using a 3 mL syringe (FORTUNA OPTIMA Luer Lock, Poulten & Graf GmbH, Wertheim, Germany) with a nozzle (25-gauge, length 7 mm; Carl Roth GmbH & Co. KG, Germany). The syringe was loaded with different quantities of the material depending on the experiment and purged with nitrogen for 15 min using a pressure of 0.3 bar before placing it inside the head preheated at the respective temperature. The first print was performed after 1 h of heating.

2.5. Collector Configuration

All direct-writing experiments were performed with a G-code designed to automatically print fiber arrays at all the heating times. The fibers were direct-written onto microscope slides (76 mm × 26 mm × 1 mm, VWR, Radnor, Pennsylvania, USA) with two slides being used as stabilization regions and ten slides for the printing experiment. The stabilization region 1 was used for left set of five slides and region 2 was used for the right set of five slides, where the jet was stabilized by direct-writing straight fibers for 8 min. Following this, the actual printing experiment had a total of 26 × 4-line fiber arrays with increasing collector

speeds of 100 mm min⁻¹ for each array from the initial 100 mm min⁻¹ value. A schematic of the slide layout is shown in Figure S1, Supporting Information.

2.6. Identifying the Minimal Direct-Writing Temperature

The minimal direct-writing temperature for the syringe (T_{Syringe}) and the nozzle (T_{Nozzle}) of different blends were determined. Two separate temperature sweeps were used for T_{Syringe} and T_{Nozzle} where a heating rate of 5 K per slide was followed by 2 K per slide to narrow on these values. The fiber diameter consistency was determined by stereomicroscopy (Discovery V.20, Carl Zeiss AG, Oberkochen, Germany) and repeated until the direct-writing speed was reliable after 1 h of heating. The resulting T_{Syringe} and T_{Nozzle} for each blend are shown in Table 1.

2.7. Critical Translation Speed and Fiber Diameter

For jet speed determination using CTS, the same collector setup as described above was used and temperatures set according to Table 1. A collector distance of 3.5 mm, nozzle protrusion of 0.5 mm, a voltage of 5.0 (head) and -0.5 kV (collector) were used (Figure 2C). The climate chamber for the MEW printer was set to maintain a constant ambient temperature of 20 °C and relative humidity of 40%. Samples were produced after 1, 1.5, 2, 2.5, 3, 3.5, 6, 12, 18, and 24 h of heating to investigate the influence of prolonged high temperature exposure. Diameter determination was done using scanning electron microscopy (SEM)

(Crossbeam 340 SEM, Carl Zeiss Microscopy GmbH) after sputtering the samples with a 3 nm layer of platinum using a sputter coater (Leica EM ACE600, Wetzlar, Germany). The fiber diameters were determined for arrays printed at CTS and for a collector speed that was above CTS for the first 6 h of heating (v_{fix}). The second speed was chosen to simulate the usual approach to scaffold direct-writing with a constant collector speed above CTS. A total of eight images per speed were used and this procedure was repeated three times.

2.8. Mechanical Properties of Fibers

Bundles of 30 fibers were printed for each material, detached from the glass slide collector, and affixed to a cardboard frame with a gap of 4 mm (effective length) using a double-sided tape. Cyclic and pseudostatic tensile testing was performed using Bose ElectroForce 5500 (TA Instruments, New Castle, USA). The sample was attached to the tensile grips of the mechanical testing equipment and the edges of the cardboard frame were cut before initiating the tests. A strain rate of 0.05 mm min⁻¹ was used for tensile tests. For cyclic testing, the samples were pre-loaded to 50% strain at 0.05 mm min⁻¹ followed by a half sine wave with a 1 mm amplitude (total 75% strain) and 1 Hz frequency. The sample was held at this position (50% strain) for 30 s to allow elastic recovery of fibers and the cycle was repeated 10 times (Figure S3, Supporting Information). A total of nine samples (three samples for three different batches each) were tested for each blend. PLGA30 could not be used to provide data as sample handling was difficult, and it was not possible to lift fibers from the collector without damaging them. Young's modulus was calculated as the ratio of stress to strain% in the initial onset regions of the data obtained.

2.9. Videography

All videos were recorded using a Nikon Z6 digital camera with Nikon ED 200 mm lens while editing and compilation was performed in the software Blackmagic Resolve 16 (Blackmagic Design, USA).

2.10. Sample Preparation for Gel Permeation Chromatography and Differential Scanning Calorimetry

A setup like the aforementioned collector configuration was used. Instead of glass slides, glass vials were used to collect samples and the heating times before sample collection were kept the same. To keep the collection time at a minimum, a 21 G nozzle (length 7 mm; Carl Roth GmbH & Co. KG, Germany) was utilized and the syringe was filled with material to the 0.6 mL mark. To extrude the material, a pressure of 3.0 bar was applied. As the height of the glass containers was 45 cm, the head-to-collector distance was set to 60 mm and a total voltage of 6.0 kV (3.0 kV for head and -3.0 kV for collector) was applied to accelerate the collection of the viscous melt. Three samples were drawn for each material at every heating time point and the resulting samples were stored under argon at -80 °C before further analysis.

2.11. Gel Permeation Chromatography

All samples ($n = 3$) were dissolved in chloroform (Carl Roth, Karlsruhe, Germany) at a concentration of 5 mg mL⁻¹ and mixed for 2 h. The resulting solutions were then filtered through a 0.45 μm polytetrafluoroethylene filter. The measurement was carried out using a gel permeation chromatography (GPC) device from Malvern (Herrenberg, Germany) with a Viscotek GPCmax (in-line degasser, 2-piston-pump and autosampler) equipped with a column oven (35 °C), refractive index (RI) detector (Viscotek VE3580), a pre-column (Viscotek CGuard), and two columns (2× Viscotek LC4000L, length = 300 mm, width = 8 mm, porous styrene divinylbenzene copolymer, particle size 7 μm). A flow rate of 1.0 mL min⁻¹ was kept throughout the measurement. To determine the number average molecular weight (M_n) of the samples, polystyrene standards were used.

2.12. Differential Scanning Calorimetry

To determine the glass transition temperature (T_g) of the blends, approximately 10 mg per sample were encapsulated inside a pierced lid aluminum crucible (Netzsch, Selb, Germany) and measured with a differential scanning calorimetry (DSC) 204 F1 Phoenix (Netzsch, Selb, Germany). The sample was heated to 120 °C and cooled to -50 °C with 10 K min⁻¹ to eliminate any thermal history. After that, another heating cycle from -50 to 120 °C and cooling from 120 to -50 °C with 10 K min⁻¹ was measured. Samples of the neat material and all the blends were collected after 1, 2, 3, 6, 12, and 24 h and measured ($n = 3$). To determine T_g , the data were evaluated using Proteus Thermal Analysis (Netzsch, Selb, Germany, version 5.2.1) software.

3. Results and Discussion

3.1. General Jet Behavior

The addition of plasticizer significantly lowered the glass transition temperature of PLGA which could impact the jet behavior. For PLGA and PLGA10, the jet solidifies before landing, fails to attach to the collector surface and gets attracted toward the MEW head. However, this effect is reduced in PLGA20 and not observed for PLGA30 (Video S1, Supporting Information).

3.2. MEW of Neat PLGA

MEW processing of PLGA results in fibers with visually smooth surfaces and a diameter that ranges between 20.56 and 27.37 μm. A minimum temperature of 144 (T_{Nozzle}) and 165 °C (T_{Syringe}) was required to process the neat polymer. In what may initially appear as an unstable process, the fiber diameter of PLGA at the CTS becomes consistent after 3.5 h of heating. This unstable processing period sees an increase in diameter of 33% while the CTS did not change substantially. A change in the fiber diameter was also recently observed for PCL, albeit over a longer period of 5 days before stabilization for the following 25 days of heating.^[4]

The most common approach to MEW, however, is to use collector speeds that are substantially higher than the CTS—typically

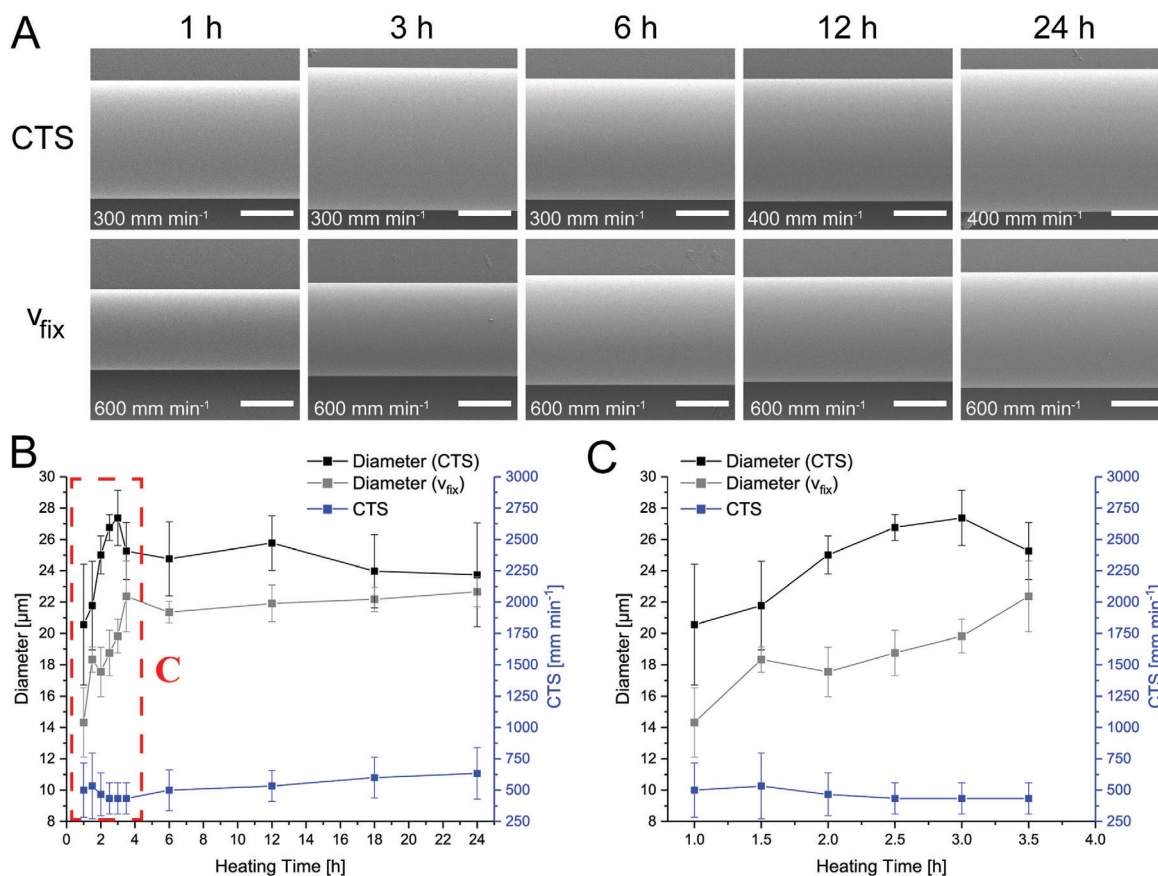


Figure 3. MEW of neat PLGA. A) SEM images of fibers printed at different time-points at CTS and v_{fix} , B) diameter and CTS development over time and C) zoomed-in version of the graph for first 3.5 h. It was observed that after 3.5 h of direct-writing PLGA stabilizes as a process. All scale bars are 10 μm .

1.1 to $1.5 \times \text{CTS}$ —so that straight lines are direct-written. **Figure 3** shows smooth, well-formed fibers of neat PLGA printed above the CTS which generally have a smaller diameter. This has previously been shown for PCL, and it is important to note for researchers who aim to direct-write non-linear fibers, that is, sinusoidal morphologies for auxetic properties.

The CTS data of PLGA are shown in **Figure 3B** with a zoomed-in graph shown in **C**. To present results that reflect the unstable and the stable processing period, the heating time was divided into two sections: up to and including the initial 3.5 h of heating and everything thereafter. Notably, the CTS for PLGA is relatively stable during this period. The cause of this CTS stability but increase in fiber diameter is not fully elucidated. A similar behavior was observed for PCL in a different study.^[4] Since the MEW process operates in a balance of many instrument parameters, changes in the properties of the processed polymer are likely to have a visible effect on the outcome.

3.3. Fiber Morphology

A smooth fiber morphology was observed for all polymer blends and was unaltered with heating time. Due to a 2600 mm min^{-1} collector speed limit for the testing routine, only the first 3 h for v_{fix} of PLGA30 is visible. The fibers degraded in quality with time

(**Figure 4A,B**) and CTS exceeded the speed limit of the test after 6 h (**Figure 4C**). The PLGA30 fibers are no longer round, but merged with the glass slide, likely caused by the reduced T_g of 4°C affecting the speed at which a solid fiber is formed. Fibers made from PLGA20 (**Figure 4D**) and PLGA10 (**Figure 4E**) also have smooth surfaces and did not appear to flatten.

3.4. CTS and Fiber Diameter

The CTS data and fiber diameters of PLGA and its blends are shown in **Figure 4C,F**, respectively. During the first 3.5 h, the CTS of PLGA10 is very stable. To quantify these values, the change in CTS with time (**Figure 4C**) is calculated by using the slope of the graph. To compare, PLGA shows a ΔCTS of $-31.6 \pm 10.8 \text{ mm min}^{-1}\text{h}^{-1}$ and PLGA10 of $-8.3 \pm 14.6 \text{ mm min}^{-1}\text{h}^{-1}$ (**Figure 4G**). In comparison, the CTS of PLGA20 and PLGA30 increases with a rate of 90.4 ± 16.9 and $241.1 \pm 44.3 \text{ mm min}^{-1}\text{h}^{-1}$. Beyond 3.5 h, the CTS increases for all blends with PLGA10 being the slowest. In contrast, the change in CTS rate for PLGA remained similar throughout the print with only a gradual increase despite an increase in fiber diameter. Graphs with further details and zoomed in view of the initial 3.5 h period of direct-writing are shown in **Figure S2**, Supporting Information.

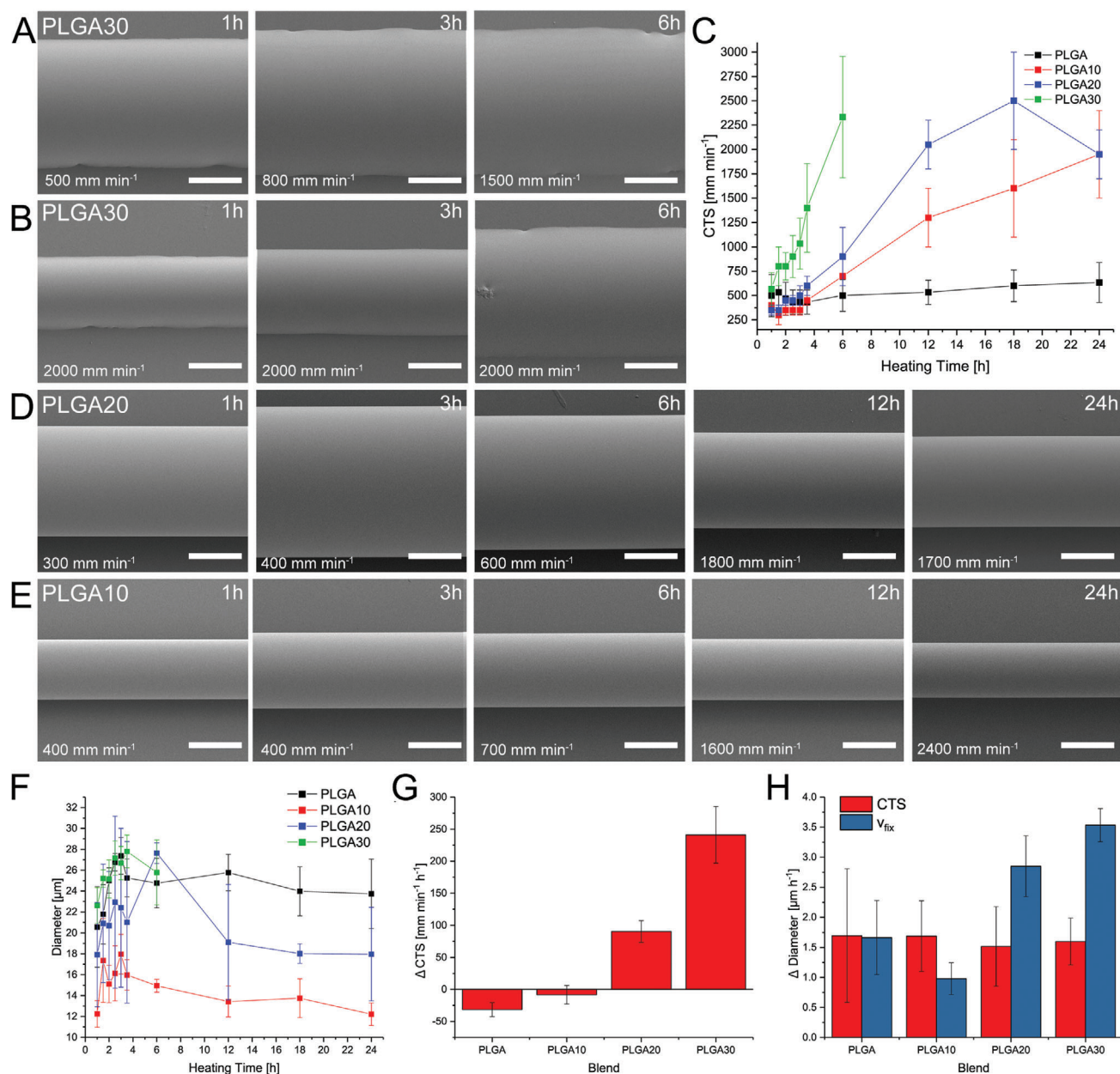


Figure 4. A,B,D,E) SEM images of fibers and changes in diameter and C) CTS for PLGA10, PLGA20, and PLGA30; F) development of the diameter at CTS. G) Δ CTS 0 to 3.5 h and H) Δ diameter at CTS and v_{fix} during the first 3.5 h of heating. All scale bars are 10 μm .

Two different speeds, CTS and v_{fix} were used for diameter determination. In the first 3.5 h of heating, all blends show an increase in the printed fiber diameter (Figure 4F). For times of 6 h and longer, the diameter was almost stable for PLGA, while PLGA10, and PLGA20 show a small decreasing trend. For PLGA30, no data could be collected beyond 6 h as the CTS was already too high to collect straight fibers. An overview of the mean fiber diameters at CTS and v_{fix} are shown in Table 2. The rate at which the diameter determined at v_{fix} is increasing follows the following order: PLGA10 ($0.98 \pm 0.26 \mu\text{m h}^{-1}$) < PLGA ($1.66 \pm$

$0.62 \mu\text{m h}^{-1}$) < PLGA20 ($2.85 \pm 0.51 \mu\text{m h}^{-1}$) < PLGA30 ($3.53 \pm 0.28 \mu\text{m h}^{-1}$) (Figure 4H).

The addition of plasticizer reduced the minimum processing temperature of the material from 165 °C (PLGA) to 157 °C (PLGA10), 155 °C (PLGA20), and 143 °C (PLGA30) (Table 1). In terms of direct-writing performance both PLGA and PLGA10 showed a negative trend in CTS progression during the first 3.5 h of processing, while CTS of PLGA20 and PLGA30 was increasing. Especially PLGA30 showed a higher rate of change in CTS, which could be explained by the GPC as PLGA30 indeed

Table 2. Mean fiber diameter values obtained for PLGA/A TEC blends at different collector speeds. Values for the initial 3.5 h of direct-writing are compared with the rest of the processing time.

Material	Initial 3.5 h		From 6 to 24 h	
	Fiber diameter (CTS) [μm]	Fiber diameter (ν_{fix}) [μm]	Fiber diameter (CTS) [μm]	Fiber diameter (ν_{fix}) [μm]
PLGA	24.28 \pm 3.35	18.63 \pm 3.09	24.45 \pm 2.67	22.03 \pm 1.03
PLGA10	16.15 \pm 2.96	14.13 \pm 1.69	13.60 \pm 1.68	14.94 \pm 0.62
PLGA20	20.99 \pm 6.92	15.85 \pm 4.44	18.79 \pm 5.55	26.92 \pm 2.97
PLGA30	25.81 \pm 2.37	18.13 \pm 4.12	25.79 \pm 3.11	25.63 \pm 0.58

degraded at a higher rate compared to the other blends. This leads to the conclusion that the plasticizer lowers the processing temperature preventing the initial fast degradation, but also seems to accelerate the degradation rate over the prolonged time period. This could be attributed to water being introduced by the plasticizer which is then causing ester hydrolysis. This makes PLGA30 to be the worst polymer candidate of the group for use in MEW fabrication as these changes in CTS are not manageable.

Even though PLGA and PLGA10 showed relatively low, and PLGA20 a manageable rate of increasing CTS, another important parameter is the fiber diameter at ν_{fix} . Measuring the fiber diameter at a constant collector speed is a good indication of changes within the material. As can be seen in Figure 4, the change in diameter with heating time is lowest for PLGA10 followed by PLGA. PLGA20 and PLGA30 both show quite high rates, which is not desired for regular scaffolds to be generated via MEW.

3.5. Mechanical Properties

Mechanical properties of the melt electrowritten fibers were assessed to study the influence of ATEC addition to PLGA. The plasticizer softened the polymeric fibers as evidenced by the Young's Modulus. PLGA fibers had the largest value of 9.13 ± 1.49 MPa with PLGA10 and PLGA20 showing values of 7.01 ± 2.35 and 0.72 ± 0.49 MPa, respectively. The samples did not fail/break for strain up to 275%. The strain recovery of samples was recorded (Video S2, Supporting Information). It was observed that PLGA underwent a plastic deformation, while PLGA10 showed some signs of partial recovery and PLGA20 showed complete recovery in ≈ 12 s (Figure 5B,C).

3.6. Gel Permeation Chromatography

GPC measurements determined the M_n changes of the different PLGA blends with heating time. The normalized data allowed better comparability between the different PLGA blends (Figure 5D). To provide further details, Figure 5E shows a zoomed-in graph for first 3.5 h. The most outstanding information is the development of the M_n of PLGA as it reduces within the first hour of heating to around 61% of the initial M_n . This initial reduction was not observed with the PLGA/A TEC blends.

3.7. Differential Scanning Calorimetry

The addition of ATEC influences the T_g of PLGA therefore DSC measurements were performed to determine the magnitude and

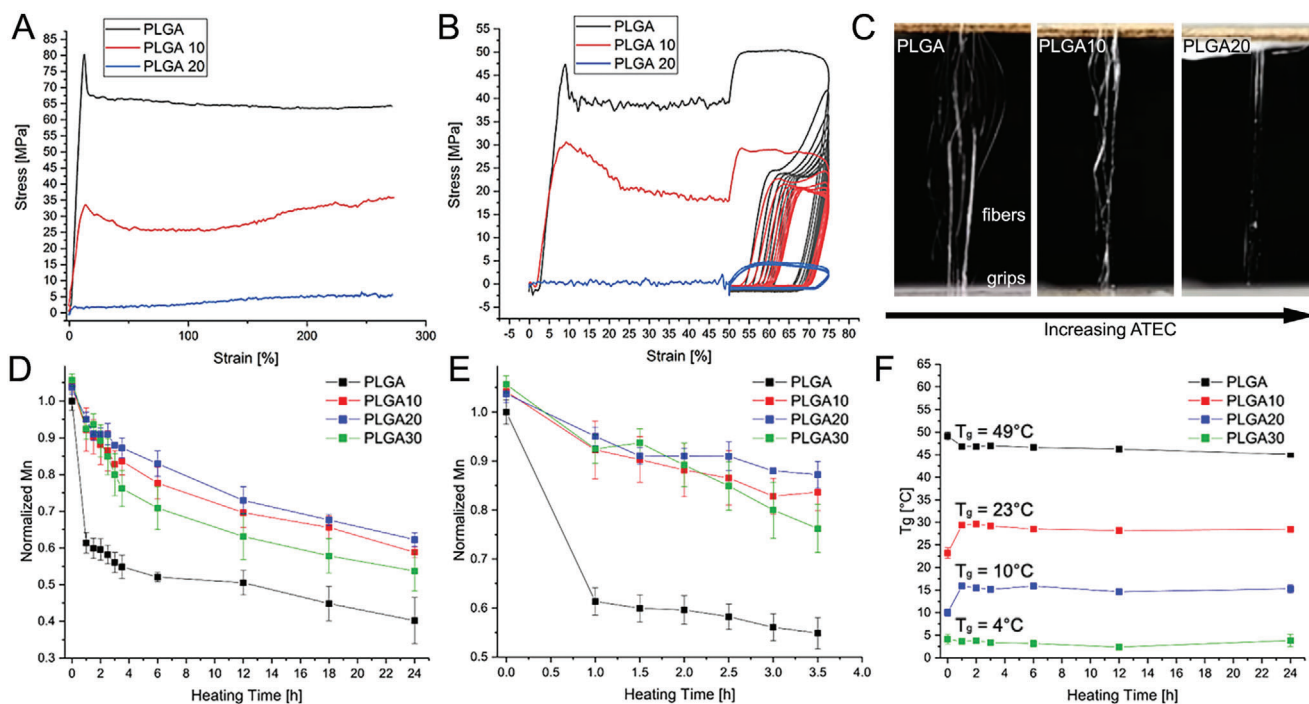


Figure 5. Stress–strain graphs for A) tensile tests and B) cyclic tests of fiber bundles (C). D) Development of the number-average molecular weight (M_n) over 24 h and E) a zoomed-in view on the first 3.5 h; F) corresponding T_g and its development with heating time.

whether this changed with time (Figure 5F). With increasing ATEC content, the T_g reduced from 49 °C (PLGA) to 4 °C (PLGA30) and then did not substantially change for the 24 h period. The T_g was found to change after the first hour of for PLGA, PLGA10, and PLGA20, reflecting the changes seen with the M_n , thermal hysteresis, also called thermal memory, could be discounted for this as it was eliminated in the experiment setup in DSC (Figure 5E,F).

3.8. Direct-Writing Interpretation

PLGA could be successfully processed into fibers using MEW, and the stability of the diameter changed primarily in the first 3.5 h of direct-writing. The CTS for PLGA is remarkably stable from beyond 3.5 h of processing (Figure 3). A possible explanation to this initial period could be given by the GPC data which showed a rapid loss in M_n in the first hour, before it reached a stable regime out to 24 h. To minimize this initial degradation, the processing temperature was lowered by preparing PLGA/ATEC blends.^[22,23] In terms of fiber morphology, there were minor differences between PLGA and its blends, except for PLGA30 where the fibers flattened with increasing processing time (Figure 3A). This could be explained by the low T_g of PLGA30 together with the heat that radiates from the printhead.

The thermal degradation of PLGA poses a challenge for its stable processing via MEW. The thermal degradation affects the time window that the melt can be stably processed, however we found in this study that a level of stability is achieved beyond 3.5 h of direct-writing, out to 24 h. Reducing this duration at which PLGA is in a molten state is desired, however it is technically challenging due to the low flow rates that MEW inherently requires. As mentioned, flow rates of 1.5–5 $\mu\text{L h}^{-1}$ have been shown to be required for MEW,^[4] even likely lower flow rates for smaller diameter fibers. Melt extrusion configurations that are proven successful such as screw-driven or even filament-driven extrusion still result in multi-hour long heating periods at such low flow rates.^[7] There is, however, potential to deliver such low flow rates to a nozzle while minimizing the heat zone with a laser system, as shown for laser melt electrospinning.^[24] This study investigates whether there are stable processing opportunities using the standard pressurized approach that the vast majority of MEW researchers use.^[1]

4. Conclusion

This study reports the first direct-writing study for the MEW of PLGA, and we observed thermal degradation within the initial processing window. After this period, the process was stable out to 24 h. A reduction of the processing temperature was achieved by the addition of the plasticizer, ATEC, and PLGA10 could be reliably printed in this initial 3.5 h period. Direct-writing above the CTS at a fixed collector speed (v_{fix}) reduced fiber diameter variability, while the addition of ATEC resulted in an elastomeric behavior of the fibers, investigated further with cyclic mechanical testing. ATEC did not substantially reduce the processing temperature, however, without significant addition of the plasticizer. It is especially recommended that future MEW studies investigate

thermal degradation behavior out to much longer times than several hours, as the initial variations in direct-writing stability may be short-lived.

Supporting Information

Supporting Information is available from the Wiley Online Library or from the author.

Acknowledgements

The technical assistance of Christian Schlör and Philipp Stahlhut is greatly appreciated as is the financial assistance from the DFG (grant #322483321). This work was supported by the Wu Tsai Human Performance Alliance and the Joe and Clara Tsai Foundation. The German Research Foundation (DFG) State Major Instrumentation Programme (INST 105022/58-1 FUGG) funded the Zeiss Crossbeam CB 340 SEM used in this study.

Open access funding enabled and organized by Projekt DEAL.

Conflict of Interest

The authors declare no conflict of interest.

Data Availability Statement

The data that support the findings of this study are available from the corresponding author upon reasonable request.

Keywords

3D printing, additive manufacturing, electrohydrodynamics, melt electrospinning writing, plasticizers, poly(lactide-co-glycolide)

Received: November 4, 2021

Revised: December 22, 2021

Published online: January 19, 2022

- [1] T. M. Robinson, D. W. Hutmacher, P. D. Dalton, *Adv. Funct. Mater.* **2019**, *29*, 1904664.
- [2] T. D. Brown, P. D. Dalton, D. W. Hutmacher, *Adv. Mater.* **2011**, *23*, 5651.
- [3] J. C. Kade, P. D. Dalton, *Adv. Healthcare Mater.* **2021**, *10*, e2001232.
- [4] C. Böhm, P. Stahlhut, J. Weichhold, A. Hrynevich, J. Teßmar, P. D. Dalton, *Small* **2021**, 2104193.
- [5] G. Hochleitner, T. Jungst, T. D. Brown, K. Hahn, C. Moseke, F. Jakob, P. D. Dalton, J. Groll, *Biofabrication* **2015**, *7*, 035002.
- [6] A. Hrynevich, B. S. Elci, J. N. Haigh, R. McMaster, A. Youssef, C. Blum, T. Blunk, G. Hochleitner, J. Groll, P. D. Dalton, *Small* **2018**, *14*, 1800232.
- [7] C. Mota, D. Puppi, M. Gazzarri, P. Bártolo, F. Chiellini, *Polym. Int.* **2013**, *62*, 893.
- [8] G. Hochleitner, T. Jungst, T. D. Brown, K. Hahn, C. Moseke, F. Jakob, P. D. Dalton, J. Groll, *Biofabrication* **2015**, *7*, 035002.
- [9] R. S. Diaz, J.-R. Park, L. L. Rodrigues, P. D. D. E. M. De-Juan-Pardo, T. R. Dargaville, *Adv. Mater.* **2021**, 2100508.
- [10] M. Castilho, D. Feyen, M. Flandes-Iparraguirre, G. Hochleitner, J. Groll, P. A. F. Doevendans, T. Vermonden, K. Ito, J. P. G. Sluijter, J. Malda, *Adv. Healthcare Mater.* **2017**, *6*, 1700311.

- [11] G. Hochleitner, M. Kessler, M. Schmitz, A. R. Boccaccini, J. Tessmar, J. Groll, *Mater. Lett.* **2017**, 205, 257.
- [12] D. Nahm, F. Weigl, N. Schaefer, A. Sancho, A. Frank, J. Groll, C. Villmann, H.-W. Schmidt, P. D. Dalton, R. Luxenhofer, *Mater. Horiz.* **2020**, 7, 928.
- [13] K. K. Chereddy, G. Vandermeulen, V. Pr at, *Wound Repair Regener.* **2016**, 24, 223.
- [14] Z. Pan, J. Ding, *Interface Focus* **2012**, 2, 366.
- [15] C. E. Holy, C. Cheng, J. E. Davies, M. S. Shoichet, *Biomaterials* **2001**, 22, 25.
- [16] J. M. Anderson, M. S. Shive, *Adv. Drug Delivery Rev.* **1997**, 28, 5.
- [17] K. A. Athanasiou, G. G. Niederauer, C. M. Agrawal, *Biomaterials* **1996**, 17, 93.
- [18] G. Sivalingam, G. Madras, *Polym. Degrad. Stab.* **2004**, 84, 393.
- [19] H. Lim, S. W. Hoag, *AAPS PharmSciTech* **2013**, 14, 903.
- [20] I. Harte, C. Birkinshaw, E. Jones, J. Kennedy, E. DeBarra, *J. Appl. Polym. Sci.* **2013**, 127, 1997.
- [21] D. Wei, J. Zhao, T. Liu, Z. Wang, *J. Thermoplast. Compos. Mater.* **2016**, 29, 366.
- [22] L. V. Labrecque, R. A. Kumar, V. Dav e, R. A. Gross, S. P. McCarthy, *J. Appl. Polym. Sci.* **1997**, 66, 1507.
- [23] V. P. Ghiya, V. Dave, R. A. Gross, S. P. McCarthy, *J. Macromol. Sci., Part A: Pure Appl. Chem.* **1996**, 33, 627.
- [24] H. Xu, M. Yamamoto, H. Yamane, *Polymer* **2017**, 132, 206.